Advancing (-)-Premarineosin A as a Potent Antimalarial Therapeutic via Metabolic Engineering and Late-Stage Derivatization

Christina M. McBride[a,b,#], Morgan McCauley[a,#], Natalia R. Harris[a], Sahar Amin[a,c], Linnea Verhey-Henke[a], Awet A. Teklemichael[d], Erin N. Oliphant[e], Patricia Dranchak[e], Brian J. Curtis[a], Katherine L. Lev[a,b], Fengrui Qu[f], Harrison M. Snodgrass[g], Jared C. Lewis[g,*], James Inglese[e,h], Xin-zhuan Su[d], Filipa Pereira[a,*], David H. Sherman[a,c,f,i,*]

[a] *Life Sciences Institute, University of Michigan, Ann Arbor, Michigan 48109, USA*
[b] *Program in Chemical Biology, University of Michigan, Ann Arbor, Michigan 48109, USA*
[c] *Department of Medicinal Chemistry, University of Michigan, Ann Arbor, Michigan 48109, USA*
[d] *Laboratory of Malaria and Vector Research, National Institute of Allergy and Infectious Disease, NIH, Rockville, MD 20852, USA*
[e] *National Center for Advancing Translational Sciences (NCATS), NIH, Rockville, Maryland 20850, USA*
[f] *Department of Chemistry, University of Michigan, Ann Arbor, Michigan 48109, USA*
[g] *Department of Chemistry, Indiana University, Bloomington, Indiana 47405, USA*
[h] *Metabolic Medicine Branch, National Human Genome Research Institute, NIH, Bethesda, Maryland 20892, USA*
[i] *Department of Microbiology and Immunology, University of Michigan, Ann Arbor, Michigan 48109, USA*

[#] *These authors contributed equally.*
[*] *Corresponding author. E-mail address: davidhs@umich.edu, fpere@umich.edu, jcl3@iu.edu*

Abstract.

Despite modern preventative and curative efforts, malaria has remained a major global health crisis. In 2023 alone, malaria was responsible for an estimated 263 million cases and 597,000 deaths. To complicate this issue, the causative *Plasmodium* parasites are becoming more resistant to available therapeutics, making it difficult to treat and prevent disease progression. Hence, the discovery of new antimalarial drugs is crucial to mitigating this crisis. One promising contender is the natural product premarineosin A, an intermediate of the marineosin biosynthetic pathway that exhibits potent and selective antimalarial activity against both chloroquine-sensitive and multi-drug-resistant *Plasmodium* strains. However, its complex chemical structure and low production titers have prevented further exploration. To improve access to this promising metabolite, we identified a biosynthetic gene cluster for (-)-premarineosin A production in *Streptomyces eitanensis.* Metabolic engineering approaches increased production from trace levels to nearly 35 mg/L, which enabled semi-synthetic and biocatalytic derivatization of the (-)-premarineosin A scaffold. Late-stage C-H bromination of the B-ring resulted in a highly potent (EC_{50} < 5 nM) antimalarial compound with low cytotoxicity. These findings report progress toward the sustainable access of (-)-premarineosin A and the first structure-activity relationship study for this unique scaffold in the search for improved antimalarial therapeutics.

Introduction.

The prodiginines are a class of microbial natural products distinguished by a core tripyrrole moiety and a striking red color[1]. These metabolites have exhibited remarkable anticancer[2–4], antibacterial[5,6], antifungal[6], antimalarial[7–11], and immunosuppressant[3] properties. Cyclic prodiginines are particularly notable, as their constrained conformations encourage the binding of charged ions, leading to enhanced bioactivity compared to their straight-chained counterparts[4,12,13]. For instance, marineosin A, a cyclic prodiginine isolated from *Streptomyces* CNQ-617, incorporates a unique spiroaminal structure that confers potent cytotoxicity[14]. In a key late-stage step in marineosin A biosynthesis, the bright red 23-hydroxyundecylprodiginine (23-HUP, **1**) undergoes an oxidative bicyclization at the C8-C9 double bond catalyzed by a Rieske oxygenase (MarG) to form premarineosin A[11]. Finally, premarineosin A is converted to marineosin A by a MarA-catalyzed reduction of the C6-C7 double bond[11,14]. Premarineosin A is of particular interest, as it exhibits single-digit nanomolar antimalarial activity *in vitro* and is notably less cytotoxic than marineosin A[11].

Due to emerging drug resistance, developing new antimalarials that match or exceed the efficacy of current therapeutics is paramount[15,16]. Various prodiginine analogs have been generated to improve their antiplasmodial and cytotoxic properties[7–10,17,18]. Most often, total synthesis has been employed to derivatize linear prodiginines, with modifications occurring early in the route through the functionalization of simple precursors[9]. Due to the synthetic complexity of the spirocyclic core, premarineosin A is significantly less amenable to total synthesis, as evidenced by all prior efforts resulting in low overall yields[19,20]. Synthesis of premarineosin A analogs has been attempted via bioconversion of 23-HUP, but is limited by low conversion rates[7]. Heterologous expression of the marineosin biosynthetic cluster disrupted in *marA* in *Streptomyces venezuelae* enabled the isolation of 0.5 mg of premarineosin A[11]. However, no production was observed in cultures >100 mL, limiting further structural characterization, derivatization, and drug development efforts.

In this work, we report a previously unexplored (-)-premarineosin A (**2**) (*pma*) biosynthetic gene cluster (BGC) in *Streptomyces eitanensis* and employed pathway engineering to improve its production. Access to a sustainable source of **2** enabled us to develop high-yield strategies for the late-stage derivatization of (-)-premarineosin A via unique semi-synthetic and biocatalytic approaches. The new (-)-premarineosin A derivatives were investigated for potency and toxicity *in vitro*, which identified a novel brominated analog with high potency against the *Plasmodium falciparum* parasites.

Results.

Genome and metabolome analysis identified a (-)-premarineosin A biosynthetic gene cluster in *S. eitanensis*. Recently we observed the production of 23-hydroxyundecylprodiginine in a *Streptomyces eitanensis* strain which was engineered for improved production of concanamycin A.[21] Close inspection of the strain genome revealed a biosynthetic gene cluster (BGC) with 90% similarity to the canonical marineosin BGC (MIBiG: BGC0000091)[11,22]. However, it lacked the putative acyltransferase (MarE) and reductase (MarA) needed to generate the 1-pyrroline B-ring in marineosin biosynthesis (**Figure 1A-C**)[11]. Untargeted metabolomic analysis revealed the production of a compound with the same molecular weight and MS fragmentation pattern as premarineosin A, while marineosin production was not observed (**Figure S1**). Thus, we reasoned that the identified *pma* BGC likely encoded premarineosin assembly as a terminal metabolite, suggesting that *S. eitanensis* could serve as an ideal chassis strain for optimizing its large-scale production.

Overexpression of *pma* cluster-situated regulator (*pmaD*) and Rieske oxygenase (*pmaG)* improved (-)-premarineosin A production in *S. eitanensis.* Culturing wildtype *S. eitanensis* resulted in the identification of trace amounts of (-)-premarineosin A (**Figure 1D**). Annotation of the *pma* BGC revealed a predicted regulatory protein, PmaD, which is a homolog (40% protein identity, 52% similarity) of the RedD transcriptional activator from the undecylprodigiosin (UDP) pathway in *Streptomyces coelicolor* A3(2)[23]. Overexpression of *redD* in both its native host and *Streptomyces lividans* enables overproduction of UDP[23–25], suggesting that PmaD may similarly regulate (-)-premarineosin A production in *S. eitanensis*. Inspired by our previous work[21], we engineered *S. eitanensis* for enhanced (-)-premarineosin A production using a regulatory gene expression strategy. The *pmaD* gene was amplified from the *S. eitanensis* genome and used to assemble a construct in pSET152k under the strong constitutive promoter KasOp*, yielding pSET152k-*pmaD*. This plasmid was integrated at the ΦC31 actinophage integrase *attB* site in the *S. eitanensis* genome, generating the *pmaD* overexpressing strain FP10017 (**Figure S2**). To ensure that the producing phenotype was directly attributed to the overexpression of the *pma* genes, we integrated the empty vector into the *S. eitanensis* genome, generating the strain FP10016. Under non-optimized culture conditions (corn gluten meal), the FP10017 strain produced significantly more (-)-premarineosin A (14.7 ± 1.4 mg/L) than the wild-type strain (below the limit of detection) (**Figure 1D**). Production of **2** was also observed in the vector control FP10016 strain (1.0 ± 0.4 mg/L), albeit at a 14-fold lower titer than the engineered FP10017 strain.

Accumulation of 23-HUP was observed in the engineered FP10017 strain (**Figure 1D**). In the last step of (-)-premarineosin A biosynthesis, the putative Rieske oxygenase PmaG catalyzes the bicyclization of 23-HUP into **2**[7,11]. Hence, we designed the pSET152k-*pmaDG* plasmid for constitutive overexpression of *pmaG* and *pmaD in S. eitanensis* to improve (-)-premarineosin A production. This plasmid was integrated into *S. eitanensis* wildtype, yielding the FP10018 strain. Constitutive overexpression of *pmaG* with *pmaG* significantly enhanced (-)-premarineosin A production (to 23.3 ± 0.5 mg/L) in FP10018, a 1.6-fold increase compared to overexpression of *pmaD* alone. The metabolic shift toward the production of **2** is also reflected by the difference in color between the FP10016/wildtype (green) and FP10017/FP10018 (red) strains (**Figure 1E**).

Optimization of media composition and culture conditions enhances secondary metabolite production in *Streptomyces* sp[21,26–28]. In *S. eitanensis*, crude protein source was shown to have the greatest effect on secondary metabolite production[21]. While corn gluten meal (GICYE) medium resulted in optimal CMA production in *S. eitanensis*[21], we identified soybean meal as the ideal complex protein source for enhanced (-)-premarineosin A production (**Figure S3**). Large-scale (1L) cultivation of the FP10018 strain in soybean meal medium (GISYE) significantly improved (-)-premarineosin A production by 1.39-fold in comparison to GICYE cultivation (**Figure 1D**). Production of **2** and **1** was assessed throughout cultivation, and while (-)-premarineosin A titers peaked around day six, the titers of 23-HUP were lowest on day seven (**Figure 1F**, **Figure S4**). Both acetone and methanol were investigated as extraction solvents, with acetone generating, on average, higher (-)-premarineosin A and 23-HUP titers (**Figure 1D**, **Figure S5**).

Under optimal conditions (soybean meal media at 22 °C for seven days followed by extraction with acetone), the engineered FP10017 and FP10018 strains produced comparable amounts of (-)-premarineosin A (34.8 + 1.6 mg/L and 33.7 + 5.1 mg/L, respectively), over 200-fold more than *S. eitanensis* wild-type (0.2 + 0.1 mg/L) (**Figure 1D**). The FP10018 strain, however, produces nearly twice ($p < 0.05$) as much **2** per dry cell weight (5.1 mg/g DCW for FP10018 vs. 2.6 mg/g DCW for FP10017) (**Figure 1F**). As with the corn gluten media, the FP10016 strain produced nearly 20-fold more **2** (3.0 + 2.1 mg/L) compared to the wildtype. We observed significantly ($p < 0.005$) increased production of the 23-HUP in the FP10018 strain when cultured in soybean meal media (**Figure 1D**). (-)-Premarineosin A was purified and structurally characterized using NMR, X-ray crystallography **(Figure 1C)**, and polarimetry. While the relative stereochemistry of (-)-premarineosin A matches previously described reports[7,13,14], our X-ray crystal data revealed that its absolute stereochemistry did not agree with the premarineosin A structure obtained by total synthesis[19,20]. As the optical rotation value for the compound (**2**) isolated in this work was $[\alpha]_D^{24}$ (c 0.4758 in MeOH) = -104.0 + 0.1°, we refer to the compound as (-)-premarineosin A.

Isolated compound **2** was tested against the drug-sensitive 3D7 and drug-resistant Dd2 *P. falciparum* parasites in an *in vitro* assay (**Table 1**). The compound was concomitantly evaluated for cytotoxicity against the HEK293 embryonic kidney and MOLT4 T-cell leukemia cell lines. (-)-Premarineosin A exhibits nanomolar potency against the 3D7 (EC_{50} = 4.0 ± 0.1 nM) and Dd2 (EC_{50} = 1.0 ± 0.7 nM) *P. falciparum* parasites with minimal toxicity to mammalian cells. In comparison, **2** is over 10- (3D7) and 350-fold (Dd2) more potent than chloroquine and is 6- (3D7) and 8-fold (Dd2) more potent than artemisinin (**Table 1**).

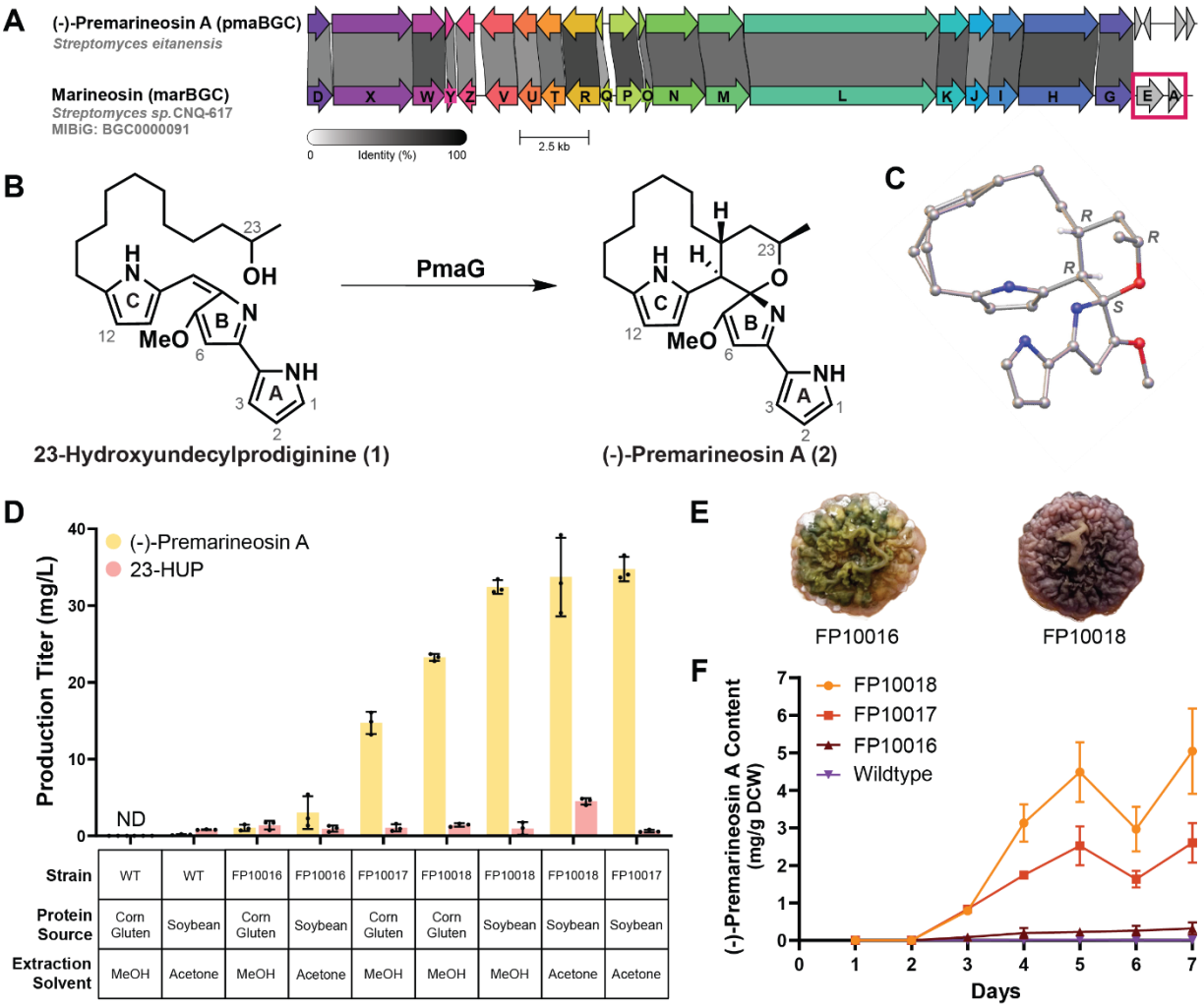

Figure 1. Overproduction of (-)-premarineosin A in *S. eitanensis*. (A) Comparison of the *S. eitanensis* (-)-premarineosin A BGC and the *Streptomyces sp.* CNQ617 marineosin BGC using clinker[29]. The (-)-premarineosin A BGC lacks genes with homology to *marA* and *marE* (red box). **(B)** The final biosynthetic step of the (-)-premarineosin A pathway. **(C)** Crystal structure of (-)-premarineosin A. **(D)** (-)-Premarineosin A (**2**) and 23-HUP (**1**) production (mg/L), quantified by AUC (HPLC) against standard curves of each compound. Dots represent three independent culture replicates. Error bars indicate standard deviation (SD). ND: Not Detected, the measured production was below the limit of detection. **(E)** Colonies of engineered FP10016 (green) and FP10018 (red) strains cultivated in solid GICYE. **(F)** (-)-Premarineosin A production (mg) per gram of dry cell weight (DCW, g) over time by wildtype and engineered FP10016, FP10017 and FP10018 strains. Error bars indicate standard deviation (SD).

Acid-catalyzed electrophilic aromatic substitution enabled late-stage derivatization of (-)-premarineosin A. With access to sufficient quantities of (-)-premarineosin A, we pursued a semi-synthetic approach to functionalize its scaffold for a structure-activity relationship analysis. Natural product analogs can and have been strategically designed to improve potency, reduce toxicity, optimize metabolism, or increase oral bioavailability in comparison to their initial scaffolds[30–34]. Ultimately, the benefit of diversifying the core premarineosin A scaffold is two-fold, offering swift access to potentially promising lead compounds while providing molecular probes for future drug target identification and elucidation of the (-)-premarineosin A mechanism of action.
Previous synthetic studies established that simple 2,5-dimethylpyrroles are susceptible to acid-catalyzed condensation with ketones, such as acetone, to form dimerized substrates at the 3-position in an electrophilic aromatic substitution-like reaction[35]. To our knowledge, this synthetic approach has not been previously applied to any natural product scaffold. Thus, we reasoned that exploration of the breadth and flexibility of this chemistry may enable access to previously untapped chemical diversity. Applying similar methodologies, we found that (-)-premarineosin A readily dimerizes under acidic conditions with both ketones and aldehydes at the C12 position of its C-ring, forming premarineosin A dimers with a gem-dimethyl-bridge (**3**), a methylene-bridge (**4**), and a trifluoromethyl-bridge (**5**) (**Figure 2A, top**). A crystal structure of **3** was obtained to confirm its unique structure, stereochemistry, and absolute configuration (**Figure 2B**).

The dimerization reaction of (**3**) with trifluoroacetone yielded a monomeric derivative (12-trifluoroacetyl premarineosin A, (**6**)), likely due to early reaction termination before complete substrate consumption (**Figure S6**). Premature termination with acetone or formaldehyde as the electrophile did not generate monomeric intermediates, suggesting that isolating these premarineosin A derivatives is only possible with bulky groups[35]. To synthesize other monomeric derivatives of (-)-premarineosin A, we used acid chlorides as the electrophile for Friedel-Crafts acylation to form 12-formyl premarineosin A (**7**) and 12-acetyl premarineosin A (**8**). Further reduction of **7** with sodium borohydride provided the desired primary alcohol, forming 12-hydroxymethyl-premarineosin A (**9**) (**Figure 2A, bottom**).

The antiparasitic activity and cytotoxicity of these synthetic derivatives were evaluated in comparison to **2** (**Table 1**). The monomeric derivatives **6**, **7,** and **8** display sub-micromolar activity against the drug-sensitive (3D7) and multidrug-resistant (Dd2) *P. falciparum* parasites. Despite the reduced activity compared to (-)-premarineosin A, derivatives **6**, **7,** and **8** perform better than chloroquine against Dd2 (EC_{50} = 382 ± 22 nM). Compound **6** is the most promising semi-synthetic derivative in terms of selectivity, displaying moderate potency against Dd2 (EC_{50} = 87 ± 15 nM) with limited apparent toxicity to HEK293 cells (EC_{50} = 3710 ± 646 nM). Compound **4** (EC_{50} = 548 ± 76 nM) and **9** (EC_{50} = 704 ± 304 nM) also exhibited sub-micromolar potency against the multidrug-resistant *P. falciparum* strain yet had limited potency against the drug-sensitive strain (**Table 1**). While synthetic modifications at the C-ring reduced the antimalarial potency of the premarineosin A scaffold, the analogs broadly exhibit decreased cytotoxicity.

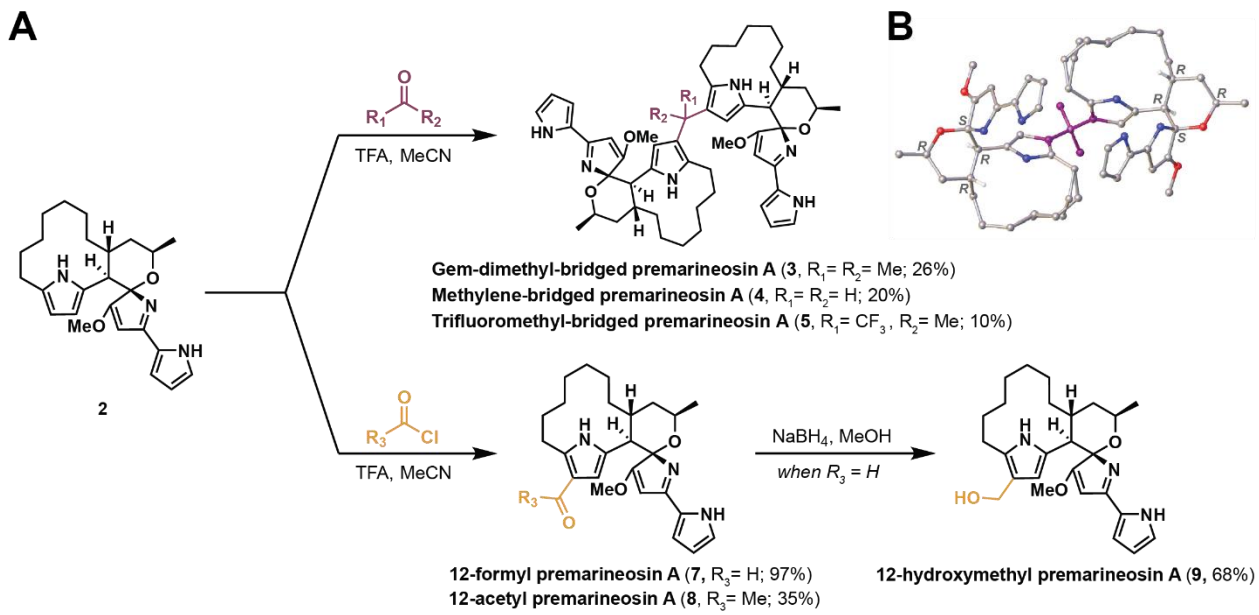

Figure 2. Semi-synthesis of premarineosin A analogs. (A) Synthesis of dimeric (top) and monomeric (bottom) premarineosin A analogs. **(B)** X-ray crystal structure of **3**.

Biocatalytic halogenation enabled late-stage C-H functionalization of (-)-premarineosin A. The biocatalytic bromination of (-)-premarineosin A represents a sustainable and innovative approach to producing novel derivatives with enhanced biological activity. Bromine holds significant value in medicinal chemistry due to its capacity to improve key pharmacokinetic properties, such as membrane permeability, target binding affinity, and metabolic stability—factors crucial for combating *Plasmodium* species effectively[36,37]. To harness the potential of selective C-H bromination of the (-)-premarineosin A scaffold, we computationally screened two bacterial flavin-dependent halogenases (FDHs). Molecular docking of **2** was performed with D3, an orphan FDH from *Saccharophagus degradans*[38], and RebH, a FDH from the rebeccamycin biosynthetic pathway[39]. While RebH shows low substrate binding and minimal contact with the active site, the D3 halogenase revealed strong substrate binding (-8.6 kcal/mol), suggesting that the enzyme may be capable of brominating the A and B pyrrole rings (**Figure 3A, B)**. Reactions of D3 with (-)-premarineosin A *in vitro* resulted in two brominated derivatives, 6-bromo premarineosin A (**10**) and 1-bromo premarineosin A (**11**), with approximately 50% substrate conversion efficiency (**Figure 3C, D**).

The antiparasitic and cytotoxic activity of brominated premarineosin A derivatives were assessed *in vitro*. 6-Bromo premarineosin A (**10**) demonstrated high potency against 3D7 (EC_{50} = 2 nM) and Dd2 (EC_{50} = 22 ± 11 nM) with low cytotoxicity (**Table 1**). Selectivity against HEK293 cells was 790 (HEK293/3D7) and 71.8 (HEK293/Dd2), while lower SI values were obtained relative to MOLT4 (337 for 3D7, and 30.6 for Dd2) (**Figure 4**). 1-Bromo premarineosin A exhibited moderate antiparasitic activity, with EC_{50} values of 53 ± 11 nM (3D7) and 61 ± 33 nM (Dd2). Despite lower activity compared to 6-bromo premarineosin A, **11** shows limited cytotoxicity against both cell lines (**Table 1**). These findings highlight 6-bromo premarineosin A (**10**) as a lead compound, combining exceptional antimalarial potency and lower cytotoxicity with remarkable selectivity.

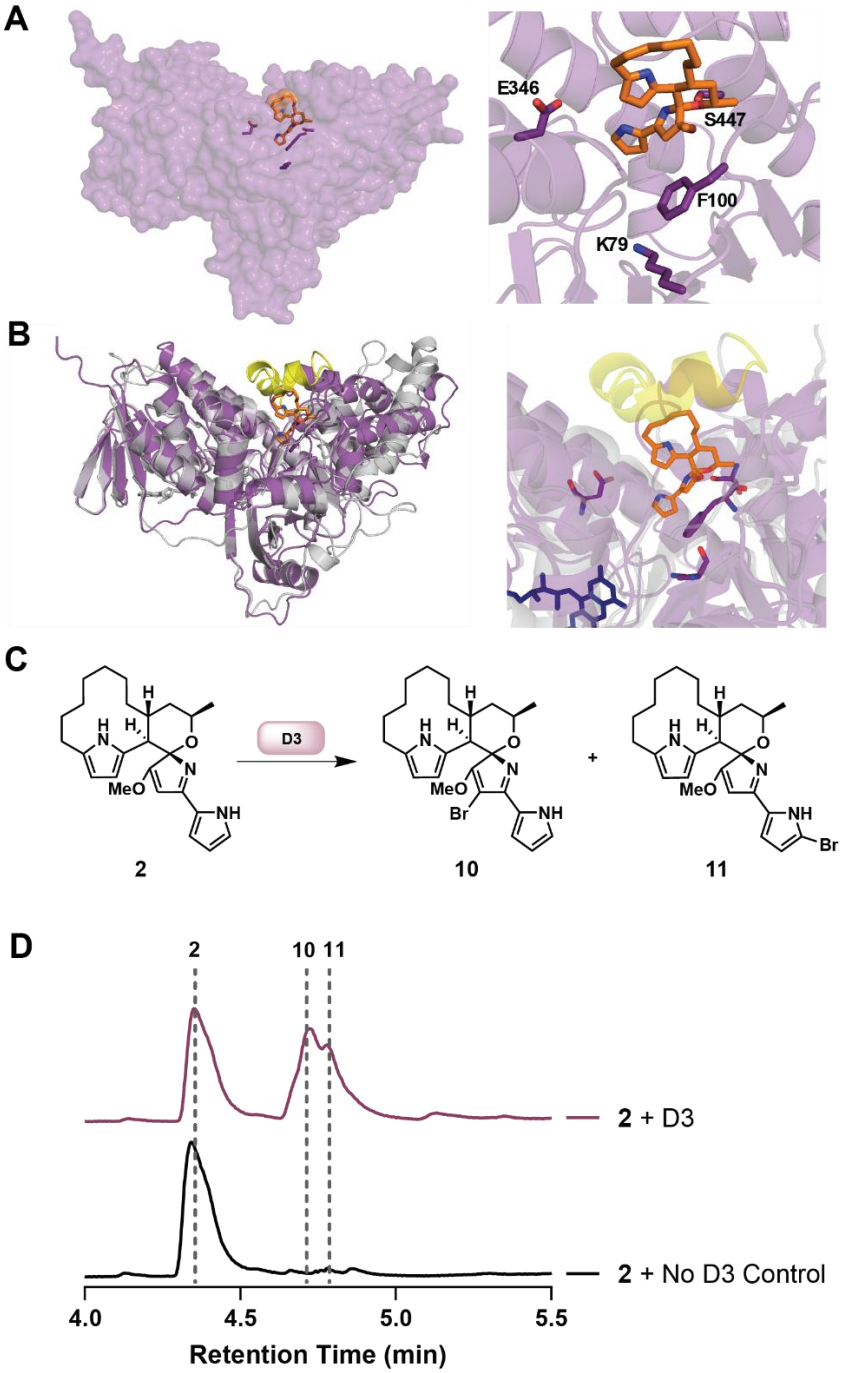

Figure 3. Biocatalytic bromination of (-)-premarineosin A. (A) In-silico docking of premarineosin (orange) docked in an AlphaFold generated model of D3's (purple) active site pocket, displaying proximity to critical residues for catalysis (Lys79 and Glu346) and selectivity (Ser447 and Phe100). **(B)** In-silico docking of premarineosin (orange) docked in an alpha-fold generated model of D3's (purple) active site pocket overlayed with a D3 homolog, RebH (grey). Premarineosin observes less favorable docking with RebH due to the active site cap (yellow) compared to D3's large open active site. **(C)** (-)-Premarineosin A is converted into two brominated products by the flavin-dependent halogenase D3. **(D)** LC/TOF traces of D3 and control reactions. Peaks corresponding to the molecular weights of monobrominated premarineosin A appear on LC/TOF traces post-reaction.

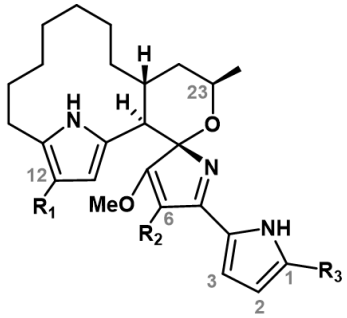

Compound	R_1	R_2	R_3	In vitro antiparasitic activity EC_{50} ± SD (nM) *Plasmodium falciparum* 3D7	Dd2	In vitro cytotoxicity, EC_{50} (nM) ± SEM HEK293	MOLT4
(-)-Premarineosin A (**2**)	H	H	H	4.0 ± 0.1	1.0 ± 0.7	1120 ± 14	1150 ± 23
Gem-dimethyl-bridged premarineosin A (**3**)		H	H	1894 ± 243	1240 ± 168	6040 ± 182	2560 ± 45
Methylene-bridged premarineosin A (**4**)		H	H	1392 ± 265	548 ± 76	4120 ± 1040	914 ± 64
Trifluoromethyl-bridged premarineosin A (**5**)		H	H	5073 ± 1000	2320 ± 448	8230 ± 190	9080 ± 581
12-trifluoroacetyl premarineosin A (**6**)		H	H	203 ± 10	87 ± 15	3710 ± 646	2300 + 1050
12-formyl premarineosin A (**7**)		H	H	165 ± 55	222 ± 53	4570 ± 1050	5150 + 348
12-acetyl premarineosin A (**8**)		H	H	178 ± 25	180 ± 14	3920 ± 672	3940 ± 1420
12-hydroxymethyl premarineosin A (**9**)		H	H	1226 ± 530	704 ± 304	7950 ± 3010	9280 + 3400
6-bromo premarineosin A (**10**)	H	Br	H	2 ± 0	22 ± 11	1580 ± 233	674 ± 3
1-bromo premarineosin A (**11**)	H	H	Br	53 ± 11	61 ± 33	2200 ± 213	2120 ± 54
Chloroquine	-	-	-	41 ± 3	382 ± 33	NA	NA
Artemisinin	-	-	-	24 ± 6	8 ± 2	NA	NA

Table 1. Bioactivity of (-)-premarineosin A (**2**) and derivatives (**3-11**). Compounds were evaluated against 3D7 (chloroquine-sensitive) and Dd2 (multidrug-resistant) *P. falciparum* strains for antimalarial activity and the HEK293 embryonic kidney and MOLT4 T-cell leukemia lines for mammalian cell cytotoxicity (72 h treatment). Selectivity Index (SI) = Mammalian Cell Line EC_{50} / *P. falciparum* EC_{50}. NA: Not assessed.

Discussion.

This work presents expanded efforts that highlight premarineosin A as a promising scaffold for malaria parasite inhibition *in vitro*. While the nanomolar potency of premarineosin A was initially reported over ten years ago, further investigation of its pharmacologic potential has been stymied by limited access to the molecule[7,11,19]. Here, we reported the identification of a (-)-premarineosin A BGC in *S. eitanensis*. By pairing genome engineering and culture optimization strategies, we increased (-)-premarineosin A titer over 200-fold (from 0.2 + 0.1 mg/L to 34.8 + 1.6 mg/L) in comparison to *S. eitanensis* wildtype. This is the highest titer reported to date, as previous heterologous expression efforts resulted in less than 5 mg/L (-)-premarineosin A[11]. While the difference in (-)-premarineosin A levels between the engineered FP10017 and FP10018 strains under optimized conditions was not statistically significant, we did observe that FP10018 produces nearly twice as much **2** per gram of dry cell weight. As the accumulation of (-)-premarineosin A and 23-HUP might inhibit cell growth, we reason that further culture optimization or adaptive laboratory evolution to increase cell viability in the engineered FP10018 strain would enhance production titers. Interestingly, the strain integrating the empty vector (FP10016) produced nearly 20-fold more (-)-premarineosin A than the wildtype. Prodiginine production in the engineered FP10016 strain could be a result of plasmid integration at the ΦC31 integrase (*attB*) site, which has been shown to alter the availability of malonyl-CoA and acetyl-CoA[40] and induce a stress response[41], stimulating secondary metabolite production.

The stereocenters of the (-)-premarineosin A isolated in this work have the same relative configuration as previously reported structures of premarineosin A from both natural product isolation[7,11,14] and total synthesis[19,20] studies. However, our crystal structures for (-)-premarineosin A and the gem-dimethyl-bridged dimer (**3**) support an absolute stereochemistry of *8S, 9R, 21R, 23R*, which is the enantiomer of the previously reported absolute structure[19] (**Figures 1C, 2B**).

The *pma* pathway engineering approach reported here provided a sustainable source of **2** that enabled semi-synthetic derivatization of the (-)-premarineosin A scaffold, culminating in the synthesis of seven new analogs. Our strategy focused on diversifying the C12 position of the (-)-premarineosin A C-ring and the surprising discovery of pyrrole dimerization chemistry with the natural product. While electrophilic substitution has been utilized previously to functionalize the β-position of pyrroles[42,43], to our knowledge this chemistry has not been explored with any natural product scaffold. Thus, the current work revealed the robust nature of acid-catalyzed electrophilic aromatic substitution of (-)-premarineosin A and a potential road map for the derivatization of prodiginines and other pyrrole-containing natural products. Of the seven semi-synthetic premarineosin A derivatives (**3-9**), five show sub-micromolar potency against the chloroquine-resistant *P. falciparum* Dd2, with three having a lower EC_{50} than chloroquine (**Table 1**). However, they all have reduced bioactivity compared to **2**, suggesting that the C12 position is crucial for the potent antimalarial activity of the premarineosin A scaffold (**Figure 4**). Remarkably, all seven synthetic premarineosin A analogs are overall less cytotoxic than **2**, in agreement with the bioactivity of other C-ring functionalized prodiginines[44–46]. Hence, functionalizing the C12 position of the C-ring is an encouraging avenue to increase the selectivity index (SI) of premarineosin A and improve its therapeutic potential. Nevertheless, we have yet to identify alternative groups to functionalize C12 that could maintain or enhance the antimalarial activity of **2**.

To modify (-)-premarineosin A beyond the C12 position (at the A- and B-rings), we explored late-stage biocatalytic C-H bromination utilizing FDHs to modify complex pyrrole-containing scaffolds. While previous studies have demonstrated the utility of FDHs like PrnC for the selective early-stage halogenation of simple pyrroles, such efforts have been limited to significantly smaller precursor molecules, including the chemoenzymatic generation of site-selective derivatives like a chlorinated analog of Fludioxonil[47]. Notably, no prior work has explored the enzymatic bromination of complex pyrrole scaffolds. As such, our application of the orphan FDH D3 from *S. degradans* to selectively brominate (-)-premarineosin A on both the spiroaminal (B-ring) and minimally substituted (A-ring) pyrroles with approximately 50% substrate conversion efficiency indicates significant promise of this strategy for expanding the scope of enzymatic halogenation (**Figure 3D**). The flexibility of this monobromination observed with D3 highlights the enzyme's capacity to target multiple distinct pyrrole rings within the (-)-premarineosin A scaffold. The observed selectivity supported computational docking studies with the AlphaFold-generated structure of D3 exhibiting strong substrate binding and a preference for bromination at the A- and B-rings (**Figure 3A**). This specificity likely arises from the structural features of D3, particularly its large and flexible active site pocket, which can accommodate the bulky (-)-premarineosin A framework (**Figure 3A**).

The 6-bromo (**10**) and 1-bromo (**11**) derivatives were substantially more potent (over 17-fold and 6-fold, respectively) than chloroquine against the multidrug-resistant *P. falciparum Dd2 strain,* underscoring their potential as lead compounds for antimalarial drug development. While neither outperformed the outstanding potency and selectivity of (-)-premarineosin A against Dd2, 6-bromo premarineosin A was twice as potent as **2** against the drug-sensitive *P. falciparum* 3D7 with improved selectivity relative to HEK293 mammalian cells (**Figure 4, Table 1**). As this potency also exceeds the efficacy of both artemisinin and chloroquine in 3D7, these results suggest that **10** is a promising therapeutic candidate for the treatment of this parasite. 1-Bromo premarineosin A also exhibited comparable potency to chloroquine against the drug-sensitive *P. falciparum* 3D7 and was less cytotoxic than **2** against both cell lines but had decreased selectivity overall. Together our results suggest that modifications at the B-ring position might be key for decreasing cytotoxicity while maintaining the single-digit nanomolar potency of (-)-premarineosin A against *P. falciparum*. Interestingly, modification of B-ring in linear prodiginines also improved selectivity against malarial parasites[9].

This study demonstrates the value of biocatalytic halogenation as a powerful tool in medicinal chemistry, offering opportunities to enhance drug efficacy, stability, and bioavailability[48]. Bromine's unique physicochemical properties, including its ability to modulate target binding affinity and metabolic stability, make it particularly valuable in antimalarial drug discovery[49]. The ability to flexibly brominate (-)-premarineosin A opens the door to systematic C-H diversification of its structure, providing a platform for the development of derivatives with tailored bioactivity against *Plasmodium* species. The remarkable selectivity of 6-bromo-premarineosin A (**10**) against *P. falciparum* (**Figure 4**) warrants further investigation into its mechanism of action and *in vivo* efficacy studies. By integrating strain engineering, biocatalysis, computational modeling, and semi-synthesis, this work lays a foundation for further rational design of next-generation antimalarial agents, harnessing the full potential of the premarineosin A scaffold to address the persistent global health challenge.

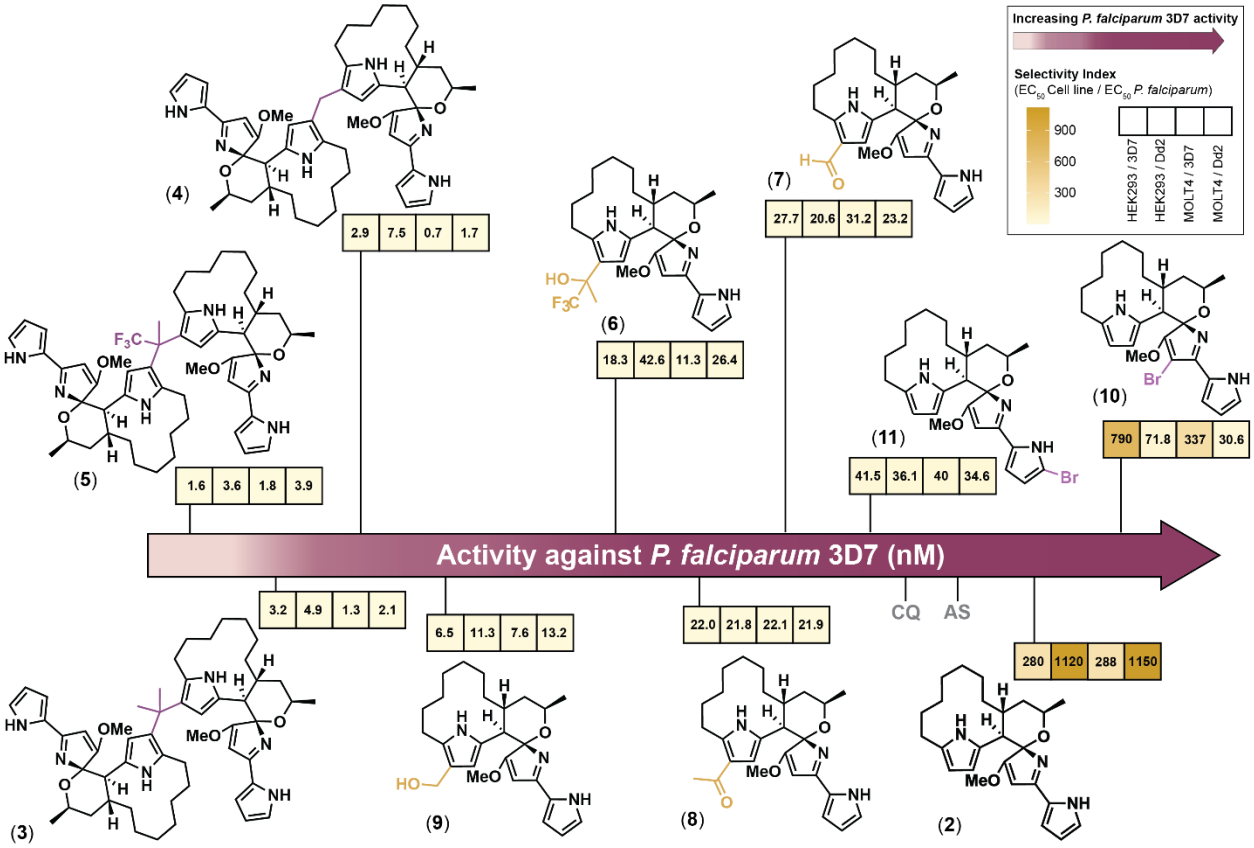

Figure 4. Selectivity index and activity of (-)-premarineosin A and analogs. Compounds were tested against 3D7 (chloroquine-sensitive) and Dd2 (chloroquine-resistant) *P. falciparum* strains for antimalarial activity and the HEK293 embryonic kidney and MOLT4 T-cell leukemia cell lines for cytotoxicity to mammalian cells. Selectivity Index (SI) = EC_{50} Mammalian Cell Line / EC_{50} *P. falciparum.*

Materials and Methods.

Strains and culture conditions. All strains that were designed and/or cultured in this work are listed in **Table S1.** Plasmid assembly, replication, and preservation were performed using high-efficiency *Escherichia coli* DH5α (NEB). *E. coli* S17-1 was used as the mobilization host for conjugation with *S. eitanensis*. All *E. coli* strains were cultivated in LB medium (10g/L tryptone, 10 g/L NaCl, and 5 g/L yeast extract in ultrapure water) at 37 °C. The LB media was supplemented with 50 µg/mL kanamycin for plasmid maintenance and selection. All *Streptromyces* strains were cultivated in 2xYT (16 g/L tryptone, 10 g/L yeast extract, and 5 g/L NaCl in ultrapure water) or peanut meal & starch media (10 g/L glucose, 30 g/L starch, 5 g/L bacto peptone, 10 g/L peanut meal, 5 g/L yeast extract, 2 g/L $CaCO_3$ in ultrapure water) for three days at 28 °C for seed culture. Strains were sporulated in OPAH (1 g/L oatmeal, 1 g/L pharmamedia, 1 g/L arabinose, 0.5 g/L humic acid, 0.5 mM KH_2PO_4, 0.5 mM $CaCl_2$, 0.5 mM $MgSO_4$, 1.9 mg/L Na_2-EDTA·$2H_2O$, 1.4 mg/L $FeSO_4$·$7H_2O$, 0.2 mg/L H_3BO_3, 0.05 mg/L $MnSO_4$·H_2O, 0.01 mg/L $ZnSO_4$·$7H_2O$, 0.01 mg/L Na_2MoO_4·$2H_2O$, 0.01 mg/L $CuSO_4$, and 0.01 mg/L $CoCl_2$ in ultrapure water). Media was supplemented with 50 µg/mL kanamycin (Goldbio, K-120-25) and/or 25 µg/mL nalidixic acid (Cayman, 19807) as needed.

Plasmid design and genome editing. All plasmids generated in this study are described in **Table S2**. The *pmaD* and *pmaG* genes were amplified from wildtype *S. eitanensis* gDNA, then assembled via Gibson Assembly in the plasmid pSET152k-*kasOp** between the BamHI and EcoRI restriction sites (New England Biolabs, R0136S and R0101S), as previously described[22]. Synthetic ribosomal binding sites[45] were used as overlapping regions for multi-gene vector design. Primers were designed with guidance from pyDNA[46] (**Table S3**). An integrative system, mediated by the *att*P site of the *Streptomyces* phage ΦC31[43], was used for constitutive overexpression in *S. eitanensis.* Interspecies conjugation was performed to transfer DNA from *E. coli* S171 to S. eitanensis. Following incubation (12 h, 28 °C), the plates were overlaid with 1 mL sterilized water with 1.25 mg kanamycin and 0.5 mg nalidixic acid. After 3–5 days, recombinants were transferred to OPAH plates with 25 µg/mL nalidixic acid and 50 µg/mL kanamycin. The engineered antibiotic-resistant strains were whole-genome sequenced. Cluster comparison and visualization were performed with clinker[47] and DNAviewer[48] to confirm genome integration.

Genome extraction, sequencing, and assembly. High-quality genomic DNA was prepared using reagents from the MasterPure Complete DNA and RNA Purification Kit (Lucigen, MC85200). The wildtype and engineered *Streptomyces* strains were cultivated in 2xYT for three days at 28 °C. Cells were pelleted via centrifugation, resuspended in 480 µL EDTA (50 mM, pH 8, sterile filtered) and 120 µL lysozyme (10 mg/mL, DotScientific DSL38100-10) then incubated for 35 min at 37 °C. Post-incubation, the cells were centrifuged (1 min, 17,000 x g, RT) and resuspended in 200 µL MasterPure Tissue and Cell Lysis Solution treated with 1 µL Proteinase K (Qiagen RP107B-5). Cells were incubated for 15 min at 65 °C, incubated for 2 min at 95 °C, then cooled to RT. 30 µL of RNase A (10 mg/mL, Sigma Aldrich R5503-1G) was added prior to incubation (1.5 hr, 37 °C). The genomic DNA was precipitated following the MasterPure Kit Precipitation of Total Nucleic Acids protocol. Genomic DNA quality was assessed using gel electrophoresis. *S. eitanensis* bacterial genome sequencing was performed by Plasmidsaurus using Oxford Nanopore Technology with custom analysis and annotation.

Premarineosin production conditions. Spores from OPAH plates were inoculated into 50 mL of peanut meal & starch media (10 g/L glucose, 30 g/L starch, 5 g/L bacto peptone, 10 g/L peanut meal, 5 g/L yeast extract, 2 g/L $CaCO_3$ in ultrapure water) and incubated (three days, 28 °C, 200 rpm). 10 mL of this pre-inoculum culture was used to inoculate 1 L of producing media: GICYE (10 g/L glucose, 30 g/L inulin, 5 g/L bacto peptone, 10 g/L corn gluten meal, 5 g/L yeast extract, 2 g/L $CaCO_3$ in ultrapure water, adjusted to pH=7.0) or GISYE (10 g/L glucose, 30 g/L inulin, 5 g/L bacto peptone, 10 g/L soybean meal, 5 g/L yeast extract, 2 g/L $CaCO_3$ in ultrapure water, adjusted to pH=7.0) in 2.8 L Fernbach flasks. Cultures were incubated for seven days at 22 °C and 170 rpm.

Sample preparation and quantification of premarineosin. Quantification of (-)-premarineosin A production in 1 L cultures was performed by extracting 1 mL biomass samples from three independent replicates. Biomass was collected and extracted every day for seven days to estimate production over time. Compound quantification is from extracts collected on day seven unless stated otherwise. On each collection day, 1mL was collected from each 1 L culture and

the biomass was pelleted via centrifugation (4 min, 20800 rpm, RT). The cell pellet was resuspended in 1 mL of solvent (methanol or acetone) and 100 µL of glass beads. Supernatant was combined 50:50 with solvent and stored at -20 °C until quantification. Tubes were vortexed (2 hours, 4 °C), followed by centrifugation (4 min, 20800 rpm, RT). The supernatant was retained as the extract and was stored at -20 °C until quantification. Quantification of (-)-premarineosin A production was performed using analytical HPLC (Shimadzu) equipped with a PDA detector and analyzed with a Phenyl-Hexyl column (Luna 5 µM Phenyl-Hexyl 100 Å, LC Column 250 x 4.6mm, heated to 40 °C). Water + 0.1% Formic Acid (A) / Acetonitrile + 0.1% Formic Acid (B) (10% to 100% B) was used for the mobile phase at 2 ml/min. Calibration curves were prepared with known concentrations of pure (-)-premarineosin A and 23-HUP. Production titers were determined by comparing the calibration curve and sample peak areas (AUC) at 346 nm ((-)-premarineosin A) and 520 nm (23-HUP). (-)-Premarineosin A and 23-HUP were detected in culture supernatants at trace levels for all tested strains. Therefore, quantifications reported in this document correspond to their intracellular concentrations. Statistical analysis and visualization were performed with GraphPad Prism v.10.2.2.

Biomass quantification. Daily 1 mL samples were collected from each of the three independent replicate cultures and vacuum filtered on a pre-dried membrane filter. The retained cells were dried in a microwave oven for 1.5 min[50]. As *S. eitanensis* is known to form small, spherical pellets in liquid culture, sampling was performed using sterile wide-bore pipette tips and serological pipettes.

Isolation and purification of (-)-premarineosin A and 23-HUP. The total biomass (from 1 L culture) was separated via vacuum filtration. Cell pellets were broken by coating the cells with 750 mL of 100% acetone and then shaking overnight. The acetone was obtained by vacuum filtration and then concentrated. The dried extract was concentrated with silica to be dry loaded for normal phase purification on a Biotage Isolera flash column system. Initial rounds of purification utilized a 40 g silica column with an ethyl acetate/hexane gradient (15-100%) with 1% acetic acid; (-)-premarineosin A eluted at 34-50% and 23-HUP eluted at 20-34%. (-)-Premarineosin A were further purified, separately on a 40 g silica column with a 3% Ammonia (7N) Methanol in DCM / hexane gradient (15-100%); (-)-premarineosin A eluted at 20-30%. 23-HUP fraction(s) were further purified using preparative thin-layer chromatography with an 100% 3% Ammonia (7N) Methanol in DCM / hexane mobile phase. Purity assessment of isolated compounds was performed using HPLC, NMR, and LC-MS/MS. All samples for bioactivity testing were >95% pure.

NMR data of (-)-premarineosin A. ^{1}H NMR (599 MHz, Acetone) δ 13.65 (s, 1H), 12.05 (s, 1H), 9.80 (s, 1H), 7.65 (ddd, *J* = 3.3, 2.3, 1.3 Hz, 1H), 7.45 (s, 1H), 6.50 (dt, *J* = 4.0, 2.1 Hz, 1H), 6.26 (d, *J* = 1.7 Hz, 1H), 5.72 (t, *J* = 2.9 Hz, 1H), 5.52 (t, *J* = 2.9 Hz, 1H), 4.46 – 4.38 (m, 1H), 4.14 (s, 3H), 3.03 (d, *J* = 12.5 Hz, 1H), 2.69 (dp, *J* = 13.4, 4.9 Hz, 1H), 2.39 (dt, *J* = 14.8, 4.4 Hz, 1H), 2.28 (ddd, *J* = 14.8, 11.5, 3.3 Hz, 1H), 1.95 (dt, *J* = 13.8, 4.2 Hz, 1H), 1.92 – 1.83 (m, 2H), 1.70 (ddd, *J* = 14.6, 10.0, 5.2 Hz, 1H), 1.45 (d, *J* = 6.8 Hz, 3H), 1.36 (dtdd, *J* = 25.8, 18.0, 13.5, 7.1 Hz, 4H), 1.25 – 1.17 (m, 1H), 1.11 – 1.01 (m, 2H), 0.89 – 0.77 (m, 2H), 0.54 (p, *J* = 7.0 Hz, 1H). ^{13}C NMR (151 MHz, Acetone) δ 181.77 (d, *J* = 5.5 Hz), 165.87 (d, *J* = 22.6 Hz), 135.05, 134.18, 127.55,

125.09, 121.64, 114.62, 110.64, 105.99, 97.24, 93.84, 71.23 (d, *J* = 4.3 Hz), 60.92, 46.32, 38.27, 33.56, 28.70, 28.19, 27.26, 25.87, 25.23 (2 carbons), 24.82, 20.92 (d, *J* = 4.3 Hz). LC-MS: calculated for $C_{25}H_{33}N_3O_2$ [M+H$^+$] 408.265 m/z; found 408.265 m/z.

(-)-Premarineosin A derivatization general procedure. (-)-Premarineosin A was dissolved in acetonitrile (MeCN) before trifluoroacetic acid (TFA) and a carbonyl-containing substrate was added at RT. The reaction was run until TLC (50% ethyl acetate in hexanes with 1% acetic acid) showed consumption of starting material (15 min - 6 h). After completion, the reaction was diluted with ethyl acetate and washed with 1M NaOH to quench the TFA. The aqueous layer was further extracted with ethyl acetate (x3) and organics were combined, dried over sodium sulfate, filtered, and concentrated. The material then was purified through a combination of acidic and/or basic conditions. Acidic conditions: 50% ethyl acetate (with 1% acetic acid) and hexanes (with 1% acetic acid). Basic conditions: 20-50% of a (3% ammonia (7N in methanol) in DCM solution) in hexane gradient. (See SI for detailed information and NMR data.)

AlphaFold Model Generation The amino acid sequence of the flavin-dependent halogenase D3 was obtained from the Jared Lewis Lab (Indiana University) (accession number: XXXX). The sequence was used as input for AlphaFold2 (version 2.2.0) to generate a predicted three-dimensional structure of D3. The default parameters and model configuration provided by the AlphaFold2 pipeline were utilized, with a focus on the most confident prediction based on the pLDDT score. Five models were generated, and the one with the highest overall pLDDT score was selected for subsequent studies.

Homolog Structure Retrieval The crystal structure of the D3 homolog RebH (PDB ID: 2OA1) was retrieved from the Protein Data Bank. This structure was prepared for docking by removing water molecules, heteroatoms, and non-relevant ligands using PyMOL (version 2.5.0) and AutoDockTools (version 1.5.7).

Ligand Preparation The substrate, premarineosin, was drawn and minimized using ChemDraw (version 21.0) and Chem3D (version 21.0). The minimized structure was exported in PDB format and converted to PDBQT format using AutoDockTools. Protonation states of premarineosin were assigned at pH 7.4, and torsional bonds were defined to enable flexible docking.

Docking Studies Docking simulations were performed using AutoDock Vina (version 1.1.2). Both the AlphaFold-predicted D3 structure and the crystal structure of RebH were prepared for docking by adding polar hydrogens, assigning Kollman charges, and converting the files to PDBQT format using AutoDockTools. The binding site of RebH was identified based on the position of the co-crystallized substrate or ligand. For the AlphaFold model of D3, the putative binding site was identified using structural alignment with RebH and manual inspection of conserved active site residues. A grid box was defined to encompass the putative binding pocket with dimensions of 20 × 20 × 20 Å, centered on the active site. For both D3 and RebH, docking simulations were run with an exhaustiveness parameter of 8 to ensure thorough sampling of conformational space. The docking scores were recorded in kcal/mol, and the best-ranked poses were selected based on binding energy and alignment with the expected binding mode. The top docking poses were visualized using PyMOL to assess binding orientation and interactions with active site residues.

Comparative analyses of the docking poses in D3 and RebH were conducted to infer similarities and differences in substrate binding.

Expression and Purification of D3 Halogenase. For large-scale D3 halogenase (Q21N77_SACD2) production[51], 10 mL culture tubes containing 5 mL LB with kanamycin were inoculated with BL-21(λDE3) E. coli cells harboring pET28b containing the D3 halogenase gene. The cultures were incubated overnight at 37 °C, 250 rpm. The next day, 750 mL TB supplemented with kanamycin was inoculated with the entire overnight culture. The inoculated expression cultures were incubated at 37 °C, 225 rpm until OD600 was between 0.6 and 0.8. The incubator was allowed to cool to 30 °C, and gene expression was induced with 100 µM IPTG, and the expression culture was incubated for 20 hours. Cells were harvested by centrifugation at 6000×g at 4°C for 15 min, and the cell pellet was stored at -80 °C until purification of the protein. Cells were lysed via sonication with a total processing time of 5 minutes with 1 minute on/off cycles. The cell lysate was centrifugated (60,000 ×g for 25 min), and the resulting clarified lysate was transferred to a fresh 50 mL centrifuge tube and added to pre-equilibrated Ni-NTA (equilibration buffer: 20 mM phosphate, 300 mM NaCl, 10 mM imidazole pH 7.4). Clarified lysate was incubated with resin for approximately 30 minutes, at which point it was transferred to uncapped spin columns, and the lysate was allowed to flow through. The resin was washed with at least 5 CV wash buffer (20 mM phosphate, 300 mM NaCl, 25 mM imidazole pH 7.4), at which point the spin column was transferred to a new centrifuge tube, and the resin was washed with elution buffer (20 mM phosphate, 300 mM NaCl, 250 mM imidazole, pH 7.4). Eluted protein was concentrated via diafiltration using Amicon spin filters Ultra 30K MWCO spin filters and the buffer was exchanged for storage buffer (25 mM HEPES and 10% glycerol, pH 7.4). For long-term storage, proteins were immediately frozen in liquid nitrogen and stored at – 80 °C until use.

Expression and Purification of HpaC Flavin Reductase. For large-scale HpaC production, 10 mL culture tubes containing 5 mL LB with ampicillin were inoculated with BL-21(λDE3) pRare E. coli cells harboring pET21a containing the HpaC halogenase gene. The HpaC flavin reductase (phaC plasmid) was obtained from Prof. David Ballou (University of Michigan). The cultures were incubated overnight at 37 °C, 250 rpm. The next day, 750 mL TB with ampicillin was inoculated with the entire overnight culture. The inoculated expression cultures were incubated at 37 °C, 225 rpm until OD600 was between 0.6 and 0.8. The incubator was allowed to cool to 20 °C, and gene expression was induced with 100 µM IPTG, and the expression culture was incubated for 20 hours. Cells were harvested by centrifugation at 6000×g at 4°C for 15 min and the cell pellet was stored at -80 °C until purification of the protein. Cells were lysed via sonication with a total processing time of 5 minutes with 1 minute on/off cycles. The cell lysate was centrifugated (60,000 ×g for 25 min), and the resulting clarified lysate was transferred to a fresh 50 mL centrifuge tube and added to pre-equilibrated Ni-NTA (equilibration buffer: 20 mM HEPES, 300 mM NaCl, 50 µM FAD, 10% glycerol pH 7.4). Clarified lysate was incubated with resin for approximately 30 minutes, at which point it was transferred to uncapped spin columns, and the lysate was allowed to flow through. The resin was washed with at least 5 CV wash buffer (20 mM HEPES, 300 mM NaCl, 50 mM imidazole, 10% glycerol pH 7.4), at which point the spin column was transferred to a new centrifuge tube, and the resin was washed with elution buffer (20 mM HEPES, 300 mM NaCl, 500 mM imidazole, 10% glycerol pH 7.4). Eluted protein was concentrated via diafiltration

using Amicon spin filters Ultra 30K MWCO spin filters and the buffer was exchanged for storage buffer (20 mM HEPES, 100 mM NaCl, 10% glycerol pH 7.4). For long-term storage, proteins were immediately frozen in liquid nitrogen and stored at – 80 °C until use.

Analytical scale D3 Halogenase reaction conditions. Analytical reactions were performed using 20 μM D3, 45 μM HPAC flavin reductase, 100 μM FAD, 50 mM sodium bromide, and 400 μM of (-)-premarineosin A dissolved in DMSO was added and then diluted to a final volume of 250 μL with reaction buffer (10 mM HEPES, pH 7.4 containing 10% glycerol) and initiated by adding NADH (1 mM). Two control reactions were performed which included all contents except D3. Reactions were incubated at 30 °C for 4 h agitating at 600 rpm in a thermoshaker (Multithermoshaker, Benchmark) and quenched via addition 750 μL of methanol, followed by vortexing at full speed S3 for 30 s. Quenched reactions were centrifuged at 17,000 x gravity to remove insoluble material, and the supernatant was analyzed with chromatographic conditions identical to analytical reactions and were performed using an Agilent G6230B time-of-flight (TOF) mass spectrometer system operating in positive mode, monitoring a mass range of 200 to 1200 amu with ESI-MS, and UV (195−400 nm) detection. ESI conditions were set with the capillary temperature at 320 °C, source voltage at 3.5 kV, and a sheath gas flow rate of 11 L/min, and the first 1 min of flow was diverted to waste.

Preparatory scale D3 Halogenase reaction conditions. D3 was expressed as previously reported, and conversion of (-)-premarineosin A by D3 was performed under identical conditions as those used for analytical scale reactions with 500 μM of (-)-premarineosin A and a final volume of 10 mL. The reaction was quenched via the addition of 20 mL of HPLC-grade methanol, and vortexed on the highest setting for 1 minute. This mixture was then passed through a pad of Celite© and the filter cake was washed with an additional 20 mL of methanol. To purify the biocatalytic byproduct, the aqueous solution was first extracted with ethyl acetate (x3). The organics were combined, washed with brine, dried over sodium sulfate, filtered, and concentrated. The material was then passed through a silica plug to remove residual flavin using 50% ethyl acetate (with 1% acetic acid) in hexanes. The material was then further purified by pTLC using 80% (3% ammonia (7N in methanol) in DCM) in hexanes. The major top band was pure, ring A derivative (2 mg), while the major lower band was a mixture of (-)-premarineosin A and ring-B brominated material. The impure ring B derivative was further purified by HPLC with a phenyl hexyl column (5 μm, 100 Å, 250 x 10 mm). A gradient of 10-55% of acetonitrile and water, both modified with 0.1% formic acid, over 50 minutes at a flow rate of 5 mL/min.

Mammalian Cell Lines and Cell Culture. Cells were obtained from the following sources: HEK293 (ATCC, cat # CRL-1573), MOLT-4 (ATCC, cat # CRL-1582). Cell lines were routinely tested for Mycoplasma contamination with the MycoAlert PLUS *Mycoplasma* Detection Kit (Lonza Bioscience, cat # LT07) according to manufacturer protocol. Cell number and cell viability were measured using the Countess Automated Cell Counter (Invitrogen) using Trypan blue stain (Invitrogen, cat # T10282). Human embryonic kidney HEK293 cells were maintained in DMEM with high glucose and GlutaMAX (Gibco, cat # 10566016) supplemented with 10% HyClone Characterized Fetal Bovine Serum (Cytiva, cat # SH30071.03), and 100U/mL Penicillin-Streptomycin (Gibco, cat # 15140122). Human T lymphoblast MOLT-4 cells were maintained in

RPMI 1640 Medium (Gibco, cat # 11875093) supplemented with 10% HyClone Characterized Fetal Bovine Serum (Cytiva, cat # SH30071.03), 100U/mL Penicillin-Streptomycin (Gibco, cat # 15140122), and 10 mM HEPES (Gibco, 15630080). Cells were cultured in incubators maintained at 37ºC with 5% CO_2 and 95% relative humidity.

Compounds and Reagents for Cell Viability Assays. Dimethyl sulfoxide ("DMSO"; AMRESCO, cat # RGE-3070) was used as a vehicle control. Digitonin (Sigma-Aldrich, cat # D141) was prepared as a 20 mM stock solution in DMSO and stored at -30ºC for use as a cytotoxicity control. Anti-malarial Natural Products Extracts were prepared at either 10 mM or 20 mM stock solutions in DMSO.

CellTiter-Glo Cell Viability Assay (CTG). The CTG assay (Promega, cat # G7572) was used to quantify cellular ATP according to manufacturer protocols. The Multidrop Combi liquid dispenser (ThermoFisher) was used to dispense 4µL of cells into white 1536-well microplates (Corning, cat # 7464) at a density of 1500 cells/well. Plated cells were incubated overnight. Natural Products Extracts compounds were transferred into respective wells of each plate at 25 nL/well with the mosquito (SPT Labtech) in 16-pt, 1:3 titrations for a final concentration of 125 uM – 8.71 pM for compounds with a high concentration of 20 mM, or 62.5 uM – 4.36 pM for compounds with a high concentration of 10 mM. Controls were transferred into respective wells of each plate at 25 nL/well with the mosquito with a 16-pt, 1:2 titration of Digitonin for a final concentration of 125 uM – 3.81 nM. The final concentration of DMSO was 0.58%. Cells were incubated for either 24, 48, and 72 hours, after which point 3 µL/well of CTG was transferred to each plate with the BioRaptr 2.0 FRD (LetsGoRobotics). Plates were incubated for ten minutes in the dark at ambient temperature for ten minutes. Luminescence was measured using a ViewLux 1430Ultra HTS (PerkinElmer) with the following optical settings: exposure= 1 sec, gain= high, speed= slow, binning= 2X.

CTG Data Analysis. Data were normalized to 125 uM Digitonin as -100% inhibition in a row-wise manner across the plate. Normalization was performed in Excel (Microsoft) and Concentration Response Curves (CRCs) were plotted in GraphPad Prism (GraphPad Software, Inc.) with error bars representing the standard deviation of two replicate wells (**Supplemental Figure S7**).

***In vitro* antimalarial assay**. The antimalarial growth inhibition assay was performed as described previously[52]. Briefly, the Plasmodium falciparum Dd2 and 3D7 parasites were diluted to 0.75% parasitemia with 2% hematocrit, and 50 µL diluted parasites were added to each well in a 96-well plate containing 50 µL properly diluted drugs. Compounds were three-fold diluted in triplicate with concentrations ranging from 20 – 0.001 µM/10 – 0.0005 µM. The parasites were incubated with the drug at 37°C under mixed gas (5% O2, 5% CO2, and 90% N2) condition for 48 h. DNA was released from the cultured parasite and stained with SYBR green dye. The plate was placed in the dark with gentle agitation for 1 h, and signals were read in a FLUOstar OPTIMA reader (BMG Labtech, Germany). Data from the microplate reader were analyzed using Prism 9.0 software (GraphPad Software, Inc., San Diego, CA). Each *in vitro* experiment was performed in triplicate wells and repeated twice**.**

Acknowledgements.

We are grateful for support from NIH grant R35GM118101 and the Hans W. Vahlteich Professorship (to D.H.S.), start-up funding provided by the University of Michigan Life Sciences Institute (to F.P.), a National Science Foundation Graduate Research Fellowship #DGE2241144 (to C.M.M.), an NIH F-31 #5F31DA055451-03 (to N.R.H.), the University of Michigan College of Pharmacy Duellman Graduate Student Research Fund #PGG030232 (to S.A.), a Michigan Pioneer Fellowship (to B.J.C.), and an NIH F-31 #1F31AI186432-01 (to K.L.L.). This research was also supported in part by the Intramural Research Programs of the National Center for Advancing Translational Sciences, NIH under project 1ZIA TR000495-01 (to J.I.) and the Division of Intramural Research of the National Institute of Allergy and Infectious Diseases, NIH under project # ZIA AI000892-23 (to Xz.S). This work was also supported by the University of Michigan BioNMR Core Facility (U-M BioNMR). The U-M BioNMR Core is grateful for support from U-M including the College of Literature, Sciences and Arts, the Life Sciences Institute, the College of Pharmacy, and the U-M Biosciences Initiative.

References

1. Hu, D. X., Withall, D. M., Challis, G. L. & Thomson, R. J. Structure, Chemical Synthesis, and Biosynthesis of Prodiginine Natural Products. *Chemical reviews* **116**, 7818 (2016).
2. Anwar, M. M., Albanese, C., Hamdy, N. M. & Sultan, A. S. Rise of the natural red pigment 'prodigiosin' as an immunomodulator in cancer. *Cancer Cell International* **22**, 419 (2022).
3. Williamson, N. R. *et al.* Anticancer and immunosuppressive properties of bacterial prodiginines. *Future Microbiol* **2**, 605–618 (2007).
4. Klein, A. S. *et al.* Preparation of Cyclic Prodiginines by Mutasynthesis in Pseudomonas putida KT2440. *ChemBioChem* **19**, 1545–1552 (2018).
5. Alihosseini, F., Ju, K.-S., Lango, J., Hammock, B. D. & Sun, G. Antibacterial Colorants: Characterization of Prodiginines and Their Applications on Textile Materials. *Biotechnology Progress* **24**, 742–747 (2008).
6. You, Z. *et al.* Insights into the anti-infective properties of prodiginines. *Appl Microbiol Biotechnol* **103**, 2873–2887 (2019).
7. Kancharla, P., Lu, W., Salem, S. M., Kelly, J. X. & Reynolds, K. A. Stereospecific Synthesis of 23-Hydroxyundecylprodiginines and Analogues and Conversion to Antimalarial Premarineosins via a Rieske Oxygenase Catalyzed Bicyclization. *J. Org. Chem.* **79**, 11674–11689 (2014).
8. Kancharla, P., Kelly, J. X. & Reynolds, K. A. Synthesis and Structure–Activity Relationships of Tambjamines and B-Ring Functionalized Prodiginines as Potent Antimalarials. *Journal of medicinal chemistry* **58**, 7286 (2015).
9. Kumar, A. *et al.* Optimization of B-Ring-Functionalized Antimalarial Tambjamines and Prodiginines. *J. Med. Chem.* (2024) doi:10.1021/acs.jmedchem.4c02093.
10. Papireddy, K. *et al.* Antimalarial Activity of Natural and Synthetic Prodiginines. *J. Med. Chem.* **54**, 5296–5306 (2011).
11. Salem, S. M. *et al.* Elucidation of Final Steps of the Marineosins Biosynthetic Pathway through Identification and Characterization of the Corresponding Gene Cluster. *J. Am. Chem. Soc.* **136**, 4565–4574 (2014).
12. de Rond, T. *et al.* Oxidative cyclization of prodigiosin by an alkylglycerol monooxygenase-like enzyme. *Nat Chem Biol* **13**, 1155–1157 (2017).
13. Jones, B. T., Hu, D. X., Savoie, B. M. & Thomson, R. J. Elimination of Butylcycloheptylprodigiosin as a Known Natural Product Inspired by an Evolutionary Hypothesis for Cyclic Prodigiosin Biosynthesis. *J Nat Prod* **76**, 10.1021/np400531b (2013).
14. Boonlarppradab, C., Kauffman, C. A., Jensen, P. R. & Fenical, W. Marineosins A and B, cytotoxic spiroaminals from a marine-derived actinomycete. *Org Lett* **10**, 5505–5508 (2008).
15. Dereje, N. *et al.* Resurgence of malaria and artemisinin resistance in Africa requires a concerted response. *Nat Med* 1–2 (2025) doi:10.1038/s41591-024-03439-z.
16. CDC. Malaria's Impact Worldwide. *Malaria* https://www.cdc.gov/malaria/php/impact/index.html (2024).
17. Kancharla, P. *et al.* Discovery and Optimization of Tambjamines as a Novel Class of Antileishmanial Agents. *J. Med. Chem.* **67**, 8323–8345 (2024).
18. Kancharla, P. *et al.* Total Synthesis and Antimalarial Activity of 2-(p-Hydroxybenzyl)-prodigiosins, Isoheptylprodigiosin, and Geometric Isomers of Tambjamine MYP1 Isolated from Marine Bacteria. *J. Med. Chem.* **64**, 8739–8754 (2021).
19. Feng, Z., Allred, T. K., Hurlow, E. E. & Harran, P. G. Anomalous Chromophore Disruption Enables an Eight-Step Synthesis and Stereochemical Reassignment of (+)-Marineosin A. *J. Am. Chem. Soc.* **141**, 2274–2278 (2019).
20. Xu, B., Li, G., Li, J. & Shi, Y. Total Synthesis of the Proposed Structure of Marineosin A. *Org. Lett.* **18**, 2028–2031 (2016).

21. Pereira, F. *et al.* Optimized production of concanamycins using a rational metabolic engineering strategy. *Metabolic Engineering* **88**, 63–76 (2025).
22. Zdouc, M. M. *et al.* MIBiG 4.0: advancing biosynthetic gene cluster curation through global collaboration. *Nucleic Acids Research* **53**, D678–D690 (2025).
23. Takano, E. *et al.* Transcriptional regulation of the redD transcriptional activator gene accounts for growth-phase-dependent production of the antibiotic undecylprodigiosin in Streptomyces coelicolor A3(2). *Mol Microbiol* **6**, 2797–2804 (1992).
24. Malpartida, F., Niemi, J., Navarrete, R. & Hopwood, D. A. Cloning and expression in a heterologous host of the complete set of genes for biosynthesis of the *Streptomyces coelicolor* antibiotic undecylprodigiosin. *Gene* **93**, 91–99 (1990).
25. Malpartida, F. & Hopwood, D. A. Molecular cloning of the whole biosynthetic pathway of a Streptomyces antibiotic and its expression in a heterologous host. *Nature* **309**, 462–464 (1984).
26. Ferraiuolo, S. B., Cammarota, M., Schiraldi, C. & Restaino, O. F. Streptomycetes as platform for biotechnological production processes of drugs. *Applied Microbiology and Biotechnology* **105**, 551 (2021).
27. Evangelista-Martínez, Z. *et al.* Antibacterial activity of Streptomyces sp. Y15 against pathogenic bacteria and evaluation of culture media for antibiotic production. *TIP. Revista especializada en ciencias químico-biológicas* **25**, (2022).
28. Stankovic, N. *et al.* Streptomyces sp. JS520 produces exceptionally high quantities of undecylprodigiosin with antibacterial, antioxidative, and UV-protective properties. *Appl Microbiol Biotechnol* **96**, 1217–1231 (2012).
29. Gilchrist, C. L. M. & Chooi, Y.-H. clinker & clustermap.js: automatic generation of gene cluster comparison figures. *Bioinformatics* **37**, 2473–2475 (2021).
30. Barnes, E. C., Kumar, R. & Davis, R. A. The use of isolated natural products as scaffolds for the generation of chemically diverse screening libraries for drug discovery. *Nat. Prod. Rep.* **33**, 372–381 (2016).
31. Majhi, S. & Das, D. Chemical derivatization of natural products: Semisynthesis and pharmacological aspects- A decade update. *Tetrahedron* **78**, 131801 (2021).
32. Camp, D., Davis, R. A., Evans-Illidge, E. A. & Quinn, R. J. Guiding Principles for Natural Product Drug Discovery. *Future Medicinal Chemistry* **4**, 1067–1084 (2012).
33. Camp, D., Garavelas, A. & Campitelli, M. Analysis of Physicochemical Properties for Drugs of Natural Origin. *J Nat Prod* **78**, 1370–1382 (2015).
34. Pascolutti, M. & Quinn, R. J. Natural products as lead structures: chemical transformations to create lead-like libraries. *Drug Discovery Today* **19**, 215–221 (2014).
35. White, J. D. The condensation of acetone with 2,5-disubstituted pyrroles. *Chem. Commun. (London)* 711–712 (1966) doi:10.1039/C19660000711.
36. Sleebs, B. E. *et al.* Transition State Mimetics of the Plasmodium Export Element Are Potent Inhibitors of Plasmepsin V from P. falciparum and P. vivax. *J. Med. Chem.* **57**, 7644–7662 (2014).
37. Jiang, X. *et al.* Structural Basis for Blocking Sugar Uptake into the Malaria Parasite *Plasmodium falciparum*. *Cell* **183**, 258-268.e12 (2020).
38. Lewis, J. C. Identifying and Engineering Flavin Dependent Halogenases for Selective Biocatalysis. *Acc. Chem. Res.* **57**, 2067–2079 (2024).
39. Yeh, E., Garneau, S. & Walsh, C. T. Robust in vitro activity of RebF and RebH, a two-component reductase/halogenase, generating 7-chlorotryptophan during rebeccamycin biosynthesis. *Proceedings of the National Academy of Sciences* **102**, 3960–3965 (2005).
40. Talà, A. *et al.* Pirin: A novel redox-sensitive modulator of primary and secondary metabolism in *Streptomyces*. *Metabolic Engineering* **48**, 254–268 (2018).
41. Fayed, B., Younger, E., Taylor, G. & Smith, M. C. M. A novel Streptomyces spp. integration vector derived from the S. venezuelaephage, SV1. *BMC Biotechnology* **14**, 51 (2014).

42. Hunjan, M. K. *et al.* Recent Advances in Functionalization of Pyrroles and their Translational Potential. *The Chemical Record* **21**, 715–780 (2021).
43. Tsuchimoto, T. Selective Synthesis of β-Alkylpyrroles. *Chemistry – A European Journal* **17**, 4064–4075 (2011).
44. Jenkins, S., D. Incarvito, C., Parr, J. & H. Wasserman, H. Structural studies of C-ring substituted unnatural analogues of prodigiosin. *CrystEngComm* **11**, 242–245 (2009).
45. Regourd, J., Al-Sheikh Ali, A. & Thompson, A. Synthesis and Anti-Cancer Activity of C-Ring-Functionalized Prodigiosin Analogues. *J. Med. Chem.* **50**, 1528–1536 (2007).
46. Rastogi, S. *et al.* Synthetic prodigiosenes and the influence of C-ring substitution on DNA cleavage, transmembrane chloride transport and basicity. *Org Biomol Chem* **11**, 3834–3845 (2013).
47. Peh, G. *et al.* Site-selective chlorination of pyrrolic heterocycles by flavin dependent enzyme PrnC. *Commun Chem* **7**, 1–9 (2024).
48. Mendez, L., Henriquez, G., Sirimulla, S. & Narayan, M. Looking Back, Looking Forward at Halogen Bonding in Drug Discovery. *Molecules* **22**, 1397 (2017).
49. Wilcken, R., Zimmermann, M. O., Lange, A., Joerger, A. C. & Boeckler, F. M. Principles and Applications of Halogen Bonding in Medicinal Chemistry and Chemical Biology. *J. Med. Chem.* **56**, 1363–1388 (2013).
50. Borodina, I. *et al.* Antibiotic Overproduction in Streptomyces coelicolor A3(2) Mediated by Phosphofructokinase Deletion *. *Journal of Biological Chemistry* **283**, 25186–25199 (2008).
51. Snodgrass, H. M. Methods and Applications for the Identification and Directed Evolution of Biocatalysts for Chemical Synthesis. (The University of Chicago, United States -- Illinois, 2023).
52. Liu, S., Mu, J., Jiang, H. & Su, X. Effects of Plasmodium falciparum mixed infections on in vitro antimalarial drug tests and genotyping. *Am J Trop Med Hyg* **79**, 178–184 (2008).